

# Constraints on $\alpha$ -attractor inflation and reheating

**Yoshiki Ueno<sup>1</sup> and Kazuhiro Yamamoto<sup>1,2</sup>**

<sup>1</sup>Department of Physical Science, Graduate School of Science, Hiroshima University, Kagamiyama 1-3-1, Higashi-hiroshima 739-8526, Japan

<sup>2</sup>Hiroshima Astrophysical Science Center, Hiroshima University, Kagamiyama 1-3-1, Higashi-hiroshima 739-8526, Japan

**Abstract.** We investigate a constraint on reheating followed by  $\alpha$ -attractor-type inflation (the E-model and T-model) from an observation of the spectral index  $n_s$ . When the energy density of the universe is dominated by an energy component with the cosmic equation-of-state parameter  $w_{\text{re}}$  during reheating, its e-folding number  $N_{\text{re}}$  and the reheating temperature  $T_{\text{re}}$  are bounded depending on  $w_{\text{re}}$ . When the reheating epoch consists of two phases, where the energy density of the universe is dominated by uniform inflaton field oscillations in the first phase and by relativistic non-thermalised particles in the second phase, we find a constraint on the e-folding number of the first oscillation phase,  $N_{\text{sc}}$ , depending the parameters of the inflaton potential. For the simplest perturbative reheating scenario, we find the lower bound for a coupling constant of inflaton decay in the E-model and T-model depending on the model parameters. We also find a constraint on the  $\alpha$  parameter,  $\alpha \gtrsim 0.01$ , for the T-model and E-model when we assume a broad resonance reheating scenario.

---

## Contents

<b>1</b>	<b>Introduction</b>	<b>1</b>
<b>2</b>	<b>Constraint on reheating</b>	<b>2</b>
<b>3</b>	<b>Single-field <math>\alpha</math>-attractors</b>	<b>5</b>
3.1	E-model	5
3.2	T-model	6
<b>4</b>	<b>Two-phase reheating model</b>	<b>7</b>
<b>5</b>	<b>Impact on reheating scenarios</b>	<b>11</b>
5.1	Perturbative reheating	11
5.2	Broad resonance preheating	12
<b>6</b>	<b>Summary and Conclusions</b>	<b>13</b>

---

## 1 Introduction

Inflation is a key to exploring the beginning of the universe. There are various inflation models. However, recent precise observations of the cosmic microwave background and the large-scale structure of galaxies impose useful constraints on inflation models [1]. The combination of constraints on the spectral index  $n_s$  and the scalar tensor ratio  $r$  excludes the simplest single power-law potential models. A class of inflation models that is consistent with observations is the  $\alpha$ -attractor-type models, which were recently proposed in a unified manner [2–7]; they include the Starobinsky model [8, 9] (cf., [10–13]) and the Higgs inflation model [14–18].

Reheating after inflation is important for the inflation model itself as a mechanism to realise the hot big bang universe. The energy of an inflaton field is converted to thermal radiation during a reheating epoch by processes that may include the physics of particle creation and non-equilibrium phenomena. Reheating processes have been investigated in many studies (e.g., [19–26]), in which successful scenarios of preheating and subsequent thermalisation processes were discussed; however, many uncertainties still remain (see, e.g., [27, 28] for a review).

Some authors recently investigated a constraint on the reheating epoch [29–31] that uses a recent precise constraint on the spectral index  $n_s$  [1]. The authors of [29–31] investigated constraints on the e-folding number and reheating temperature depending on the effective equation-of-state parameter of the reheating epoch. In this paper, we investigate the constraint on the reheating epoch of the  $\alpha$ -attractor-type inflation models. The authors of [31] investigated the constraint on the reheating epoch in the Higgs inflation model; however, our investigations focus on a wider class of  $\alpha$ -attractor-type models, the E-model and T-model [32, 33], which are consistent with the observations.

In our investigation, our approach to a constraint on reheating differs from those of [29–31]. These previous works assume that the universe is dominated by an energy density with a constant equation-of-state parameter  $w_{\text{re}}$ . In this work, we consider a reheating epoch

consisting of two phases. The first phase is an epoch in which the energy of the universe is dominated by uniform inflaton field oscillations (the oscillation phase), and the second phase is an epoch in which the universe is dominated by relativistic but non-thermalised particles produced by decay of the inflaton field (the thermalisation phase). Our analysis constrains the e-folding number of the oscillation phase using an observation of the spectral index  $n_s$ , which we use to discuss constraints on a parameter of the inflaton potential and a coupling constant for inflaton decay depending on two reheating scenarios.

This paper is organised as follows: In section 2, we briefly review how to constrain the e-folding number of reheating and the reheating temperature using an observational constraint on the spectral index  $n_s$ . In section 3, we investigate a constraint on the reheating epoch in a single-field  $\alpha$ -attractor model, assuming that the reheating epoch is dominated by an energy component with the equation-of-state parameter  $w_{\text{re}}$ . We demonstrate that our result is consistent with previous results. In section 4, we consider a reheating epoch consisting of the two phases, i.e., the scalar field oscillation phase and the thermalisation epoch. In section 5, we discuss the impacts of our results on two reheating scenarios. Section 5 presents a summary and conclusions. We adopt the convention  $M_{\text{pl}}^2 = 1/8\pi G$ , where  $G$  is the gravitational constant.

## 2 Constraint on reheating

We briefly review how to constrain the e-folding number of reheating  $N_{\text{re}}$  and the reheating temperature  $T_{\text{re}}$  using an observational constraint on the spectral index  $n_s$  [29–31]. We consider a single-field inflation model with a potential  $V(\phi)$ , which obeys

$$\ddot{\phi} + 3\frac{\dot{a}}{a}\dot{\phi} + \frac{\partial V}{\partial \phi} = 0, \quad (2.1)$$

where the dot indicates differentiation with respect to cosmic time, and  $a$  is the scale factor determined by the Friedman equation:

$$\left(\frac{\dot{a}}{a}\right)^2 = \frac{1}{3M_{\text{pl}}^2} \left(\frac{\dot{\phi}^2}{2} + V(\phi)\right). \quad (2.2)$$

Adopting the slow-roll approximation during inflation, the above equations are approximated as

$$3H\dot{\phi} + V'(\phi) = 0, \quad (2.3)$$

$$H^2 = \frac{V(\phi)}{3M_{\text{pl}}^2}, \quad (2.4)$$

where the prime denotes differentiation with respect to  $\phi$ , and  $H = \dot{a}/a$  is the Hubble parameter. Introducing the slow-roll parameters,

$$\epsilon = \frac{1}{2} \left(\frac{M_{\text{pl}} V'}{V}\right)^2, \quad (2.5)$$

$$\eta = \frac{M_{\text{pl}}^2 V''}{V}, \quad (2.6)$$

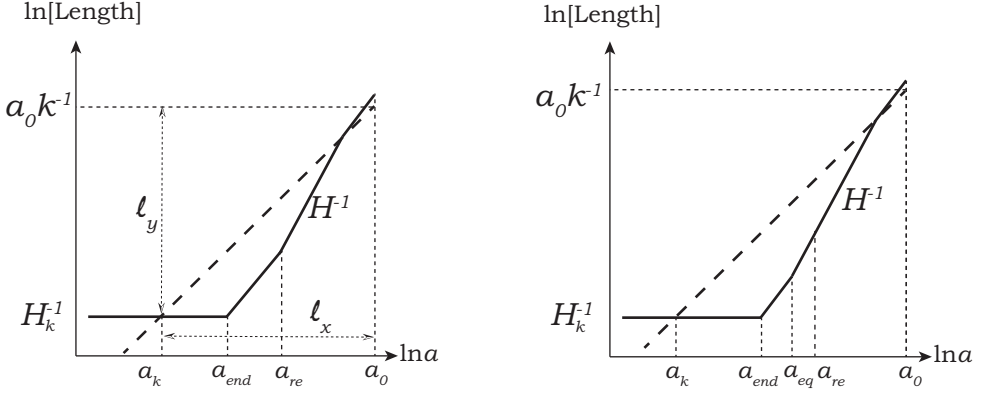


**Figure 1.** Sketch of evolution of Hubble horizon distance  $H^{-1}$  (solid curve) from the inflation epoch to the present epoch as a function of the scale factor  $a$ . Long dashed line shows the evolution of the physical wavelength of a perturbation with the comoving wavenumber  $k$ . Here a logarithmic scale is adopted for both axes.  $a_k$ ,  $a_{end}$ ,  $a_{eq}$ ,  $a_{re}$ , and  $a_0$  are the scale factors at horizon crossing during inflation, at the end of inflation, at the equal time during reheating, at the end of reheating, and at the present epoch, respectively. Left and right panels illustrate the assumptions in sections 3 and 4, respectively. In the present paper, we adopt  $k = 0.05 \text{Mpc}^{-1}$ .

we may write the the spectral index and tensor-to-scalar ratio as

$$n_s = 1 - 6\epsilon + 2\eta, \quad (2.7)$$

$$r = 16\epsilon, \quad (2.8)$$

and the energy density during the inflation epoch is written as  $\rho = (1 + \epsilon/3)V$ . We define the end of inflation as  $\epsilon = 1$ , at which the energy density of the universe can be written as

$$\rho_{\text{end}} = \frac{4}{3}V(\phi_{\text{end}}) = \frac{4}{3}V_{\text{end}}, \quad (2.9)$$

where  $\phi_{\text{end}}$  is the value of the scalar field at the end of inflation. The e-folding number between horizon crossing of a perturbation of wavenumber  $k$  and the end of inflation is estimated as

$$N_k = \ln\left(\frac{a_k}{a_{\text{end}}}\right) = -\frac{1}{M_{\text{pl}}^2} \int_{\phi}^{\phi_{\text{end}}} \frac{V}{V'} d\phi, \quad (2.10)$$

where  $a_k$  and  $a_{\text{end}}$  are the scale factors at horizon crossing of a perturbation of wavenumber  $k$  and at the end of inflation, respectively (see figure 1).

Following previous works [29–31], we first assume that during the reheating epoch, the universe is dominated by an energy component with an effective equation-of-state parameter  $w_{\text{re}}$ . At the end of the reheating epoch, we assume that the energy density of the universe is written as

$$\rho_{\text{re}} = \frac{\pi^2 g_{\text{re}}}{30} T_{\text{re}}^4, \quad (2.11)$$

where  $T_{\text{re}}$  is the reheating temperature, and  $g_{\text{re}}$  is the number of internal degrees of freedom of relativistic particles at the end of reheating, which we assume to be  $g_{\text{re}} = \mathcal{O}(100)$ . Defining

the scale factor at the end of reheating,  $a_{\text{re}}$ , then, we can write the e-folding number of the reheating epoch,

$$N_{\text{re}} = \ln\left(\frac{a_{\text{re}}}{a_{\text{end}}}\right) = -\frac{1}{3(1+w_{\text{re}})} \ln\left(\frac{\rho_{\text{re}}}{\rho_{\text{end}}}\right), \quad (2.12)$$

where  $a_{\text{re}}$  is the scale factor at the end of reheating.

Using an observational constraint on the spectral index of the initial curvature perturbations, we can constrain the e-folding number  $N_{\text{re}}$  and the effective equation-of-state parameter  $w_{\text{re}}$  of the reheating epoch. The horizon crossing of a perturbation with the wavenumber  $k$  occurs at  $a_k H_k = k$ , where  $a_k$  and  $H_k$  are the scale factor and Hubble parameter, respectively, at horizon crossing during inflation. Then, we can write

$$0 = \ln\left(\frac{k}{a_k H_k}\right) = \ln\left(\frac{a_{\text{end}}}{a_k} \frac{a_{\text{re}}}{a_{\text{end}}} \frac{a_0}{a_{\text{re}}} \frac{k}{a_0 H_k}\right), \quad (2.13)$$

where  $a_0$  is the scale factor at the present epoch. Using the definitions (2.10) and (2.12), (2.13) yields

$$N_k + N_{\text{re}} + \ln\left(\frac{a_0}{a_{\text{re}}}\right) + \ln\left(\frac{k}{a_0 H_k}\right) = 0. \quad (2.14)$$

The geometrical meaning of (2.14) is the equality in the lengths  $\ell_x = \ell_y$  in the left panel of figure 1.

From the conservation of entropy, we may write

$$\frac{a_{\text{re}}}{a_0} = \left(\frac{43}{11g_{\text{re}}}\right)^{1/3} \frac{T_0}{T_{\text{re}}}, \quad (2.15)$$

where  $T_0 = 2.725$  K is the temperature of the universe at the present epoch. Using (2.11), (2.15) is rewritten as

$$\frac{a_{\text{re}}}{a_0} = \left(\frac{43}{11g_{\text{re}}}\right)^{1/3} T_0 \left(\frac{\pi^2 g_{\text{re}}}{30\rho_{\text{re}}}\right)^{1/4}. \quad (2.16)$$

Furthermore, using (2.9) and (2.12), we have

$$\rho_{\text{re}} = \frac{4}{3} V_{\text{end}} \left(\frac{a_{\text{re}}}{a_{\text{end}}}\right)^{-3(1+w_{\text{re}})} = \frac{4}{3} V_{\text{end}} e^{-N_{\text{re}} 3(1+w_{\text{re}})}. \quad (2.17)$$

Then, the logarithm of (2.16) yields the following expression in terms of  $N_{\text{re}}$ :

$$\ln\left(\frac{a_{\text{re}}}{a_0}\right) = \frac{1}{3} \ln\left(\frac{43}{11g_{\text{re}}}\right) + \frac{1}{4} \ln\left(\frac{\pi^2 g_{\text{re}}}{30}\right) + \ln\left(\frac{3T_0^4}{4V_{\text{end}}}\right)^{1/4} + \frac{3N_{\text{re}}(1+w_{\text{re}})}{4}. \quad (2.18)$$

Using the amplitude of the scalar perturbations,  $A_s = H^4/(4\pi^2 \dot{\phi}^2)$ , and the slow-roll approximation, we may write

$$H_k = \frac{\pi M_{\text{pl}} \sqrt{r A_s}}{\sqrt{2}}. \quad (2.19)$$

Inserting (2.18) and (2.19) into (2.14), we finally have

$$N_{\text{re}} = \frac{4}{1-3w_{\text{re}}}\left[-N_k - \ln\left(\frac{k}{a_0 T_0}\right) - \frac{1}{4}\ln\left(\frac{40}{\pi^2 g_{\text{re}}}\right) - \frac{1}{3}\ln\left(\frac{11g_{\text{re}}}{43}\right) + \frac{1}{2}\ln\left(\frac{\pi^2 M_{\text{pl}}^2 r A_s}{2V_{\text{end}}^{1/2}}\right)\right]. \quad (2.20)$$

In our analysis, we adopt the amplitude of the scalar perturbation at the pivot scale  $A_s$  given by  $10^{10} A_s = e^{3.064}$  (Table 4 of [34]) and  $k = 0.05 \text{ Mpc}^{-1}$  as a pivot wavenumber. Combining (2.9), (2.12), and (2.15), we also have

$$T_{\text{re}} = \exp\left[-\frac{3}{4}(1+w_{\text{re}})N_{\text{re}}\right]\left(\frac{2V_{\text{end}}}{5\pi^2}\right)^{1/4}. \quad (2.21)$$

Because the wavenumber  $k$  and  $n_s$  are related implicitly through the scalar field  $\phi$  with  $H_k a_k = k$ , (2.7) and (2.10), one can write  $N_{\text{re}}$  and  $T_{\text{re}}$  as functions of the spectral index  $n_s$ .

### 3 Single-field $\alpha$ -attractors

In this paper, we focus on a class of single-field inflation models,  $\alpha$ -attractors in a unified manner [7], which includes Starobinsky's  $R^2$  inflation model [8, 9] and the Higgs inflation model [14–18]. This class of inflation models can be generated by spontaneously breaking the conformal symmetry [2, 4, 32, 33]. In this paper, we consider the E-model and T-model as generalised models of  $\alpha$ -attractors, which are specified by the potential (3.2) and (3.6), respectively. Starobinsky's model corresponds to the E-model with  $\alpha = 1$  and  $n = 1$  in (3.2). Single power-law inflation models are reproduced as the limit of large  $\alpha$ .

Ref. [1] demonstrates that the  $\alpha$ -attractor models are consistent with observations of the cosmic microwave background anisotropies. For consistency with the observed tensor-to-scalar ratio, roughly, we require that the parameter  $\alpha$  is less than  $\mathcal{O}(100)$ . In figures 4–6, the shaded region in each panel is excluded from the constraint on the scalar–tensor ratio. We first investigate constraints on reheating after an inflation of the E-model and T-model by following previous works [29–31]. To this end, we adopt

$$n_s = 0.9667 \pm 0.0040 \quad (3.1)$$

(see Table 4 in Ref. [34]).

#### 3.1 E-model

The E-model is specified by the potential [32, 33] written as

$$V = \Lambda^4 \left(1 - e^{-\sqrt{\frac{2}{3\alpha}} \frac{\phi}{M_{\text{pl}}}}\right)^{2n}, \quad (3.2)$$

where  $\Lambda$ ,  $n$ , and  $\alpha$  are the parameters. Using the slow-roll approximation, we find the expressions for the spectral index and the tensor-to-scalar ratio,

$$n_s = 1 - \frac{8n \left( e^{\sqrt{\frac{2}{3\alpha}} \frac{\phi}{M_{\text{pl}}}} + n \right)}{3\alpha \left( e^{\sqrt{\frac{2}{3\alpha}} \frac{\phi}{M_{\text{pl}}}} - 1 \right)^2}, \quad (3.3)$$

$$r = \frac{64n^2}{3\alpha \left( e^{\sqrt{\frac{2}{3\alpha}} \frac{\phi}{M_{\text{pl}}}} - 1 \right)^2}, \quad (3.4)$$

and for the e-foldings as functions of  $\phi$  from (2.10),

$$N_k = -\frac{3\alpha}{4n} \left[ e^{\sqrt{\frac{2}{3\alpha}} \frac{\phi_{\text{end}}}{M_{\text{pl}}}} - e^{\sqrt{\frac{2}{3\alpha}} \frac{\phi}{M_{\text{pl}}}} + \sqrt{\frac{2}{3\alpha}} \frac{\phi - \phi_{\text{end}}}{M_{\text{pl}}} \right]. \quad (3.5)$$

Thus, we can write  $T_{\text{re}}$  and  $N_{\text{re}}$  as functions of  $n_s$ , regarding  $\phi$  as an implicit parameter.

Figure 2 plots  $N_{\text{re}}$  (upper panels) and  $T_{\text{re}}$  (lower panels) as functions of  $n_s$ , where we fix  $n = 1$ . The left, central, and right panels adopt  $\alpha = 0.1, 1$ , and  $5$ , respectively. The curves in each panel represent different equation-of-state parameters  $w_{\text{re}}$ :  $-1/3$  (red curve),  $0$  (blue curve),  $1/6$  (orange curve), and  $2/3$  (green curve). Our result for  $n = 1$  is the same as that in Ref. [31].

The yellow region shows the observational constraint on  $n_s$ , (3.1). Note that for a set of the parameter  $w_{\text{re}}$ ,  $n$ , and  $\alpha$ , there appears the maximum value  $N_{\text{re}}^{(\text{max})}$  so that the curve of  $N_{\text{re}}$  is consistent with the observational constraint on  $n_s$ . For example, in the central panels, which assume  $n = 1$  and  $\alpha = 1$ , the maximum value is  $N_{\text{re}} = 8, 15, 30$ , and  $40$ , respectively, for  $w_{\text{re}} = -1/3, 0, 1/6$ , and  $2/3$ .

### 3.2 T-model

The T-model is specified by the potential [4, 32, 33]

$$V = \Lambda^4 \tanh^{2n} \left( \frac{\phi}{\sqrt{6\alpha} M_{\text{pl}}} \right), \quad (3.6)$$

where  $\Lambda$ ,  $n$ , and  $\alpha$  are the parameters. Within the slow-roll approximation, we find expressions for the spectral index, tensor-to-scalar ratio, and e-foldings as functions of  $\phi$ :

$$n_s = 1 - \frac{1}{3\alpha} \left[ 8n(1+n) \operatorname{csch}^2 \sqrt{\frac{2}{3\alpha}} \frac{\phi}{M_{\text{pl}}} + 4n \operatorname{sech}^2 \sqrt{\frac{1}{6\alpha}} \frac{\phi}{M_{\text{pl}}} \right], \quad (3.7)$$

$$r = \frac{64n^2 \operatorname{csch}^2 \sqrt{\frac{2}{3\alpha}} \frac{\phi}{M_{\text{pl}}}}{3\alpha}, \quad (3.8)$$

$$N_k = -\frac{3\alpha}{4n} \left[ \cosh \sqrt{\frac{2}{3\alpha}} \frac{\phi_{\text{end}}}{M_{\text{pl}}} - \cosh \sqrt{\frac{2}{3\alpha}} \frac{\phi}{M_{\text{pl}}} \right]. \quad (3.9)$$

Figure 3 is the same as figure 2 but for the T-model;  $N_{\text{re}}$  (upper panels) and  $T_{\text{re}}$  (lower panels) are plotted as functions of  $n_s$ , where we fix  $n = 1$ . In the left, central, and right panels,  $\alpha = 0.1, 1$ , and  $5$ , respectively. In each panel, the curves represent different equation-of-state parameters  $w_{\text{re}}$ :  $-1/3$  (red curve),  $0$  (blue curve),  $1/6$  (orange curve), and  $2/3$  (green curve).

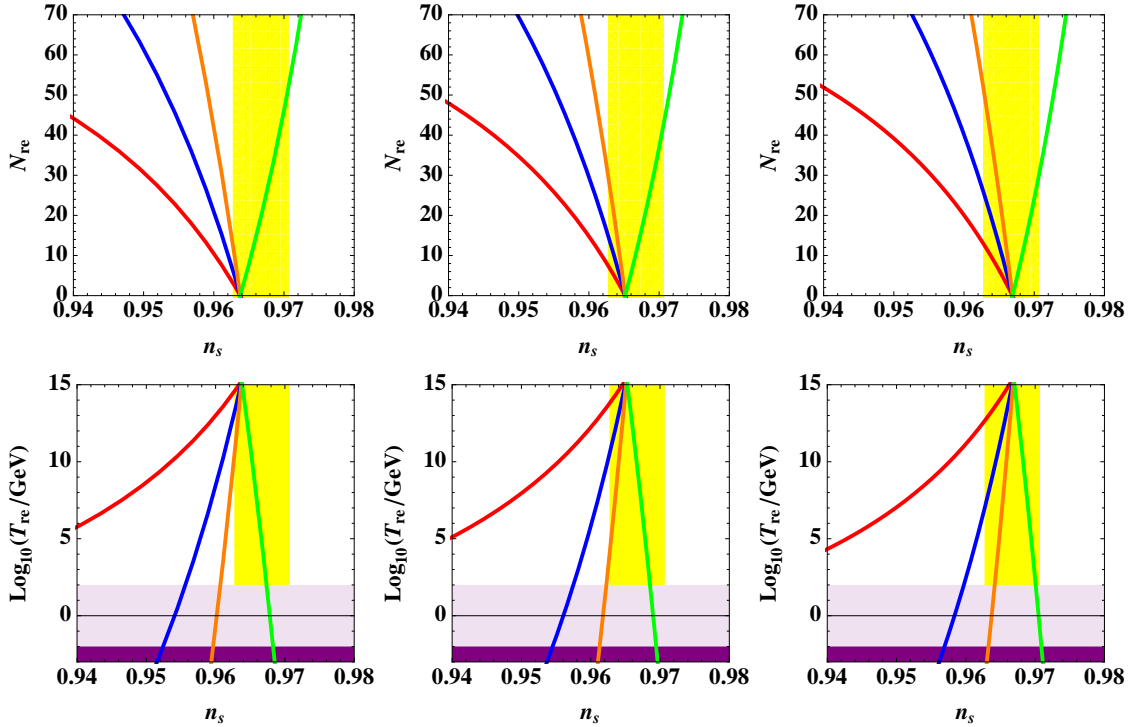


**Figure 2.**  $N_{\text{re}}$  (upper panels) and  $T_{\text{re}}$  (lower panels) as functions of  $n_s$  for E-model with  $n = 1$  and  $\alpha = 0.1$  (left panels),  $\alpha = 1$  (central panels), and  $\alpha = 5$  (right panels). In each panel, the curves represent different equation-of-state parameters  $w_{\text{re}}$ :  $-1/3$  (red curve),  $0$  (blue curve),  $1/6$  (orange curve), and  $2/3$  (green curve). Yellow regions indicate the observational constraint, (3.1). In each panel, the point at which the four curves intersect, which corresponds to instant reheating, gradually moves from left to right as the value of  $\alpha$  increases. Light purple and dark purple regions in lower panels show temperatures below the electroweak scale,  $T < 100\text{GeV}$ , and the big bang nucleosynthesis scale,  $T < 10\text{MeV}$ , respectively. For consistency with big bang nucleosynthesis,  $T_{\text{re}} \gtrsim 10\text{MeV}$ .

#### 4 Two-phase reheating model

In this section, we consider a simple scenario of reheating that consists of two phases. The first is an epoch in which the energy density of the universe is dominated by uniform oscillations of the inflaton field (the oscillation phase), and the second is an epoch in which the universe is dominated by relativistic but non-thermalised particles produced by decay of the inflaton field (the thermalisation phase). Figure 1 illustrates the difference between the assumption of this section and that of the previous section. In the oscillation phase, the scalar field and scale factor follow (2.1) and (2.2), respectively. When the scalar field oscillates around the minimum, which is approximated as

$$V = \Lambda^4 \left( \frac{2}{3\alpha M_{\text{pl}}^2} \phi^2 \right)^n \quad (4.1)$$

and

$$V = \Lambda^4 \left( \frac{1}{6\alpha M_{\text{pl}}^2} \phi^2 \right)^n \quad (4.2)$$

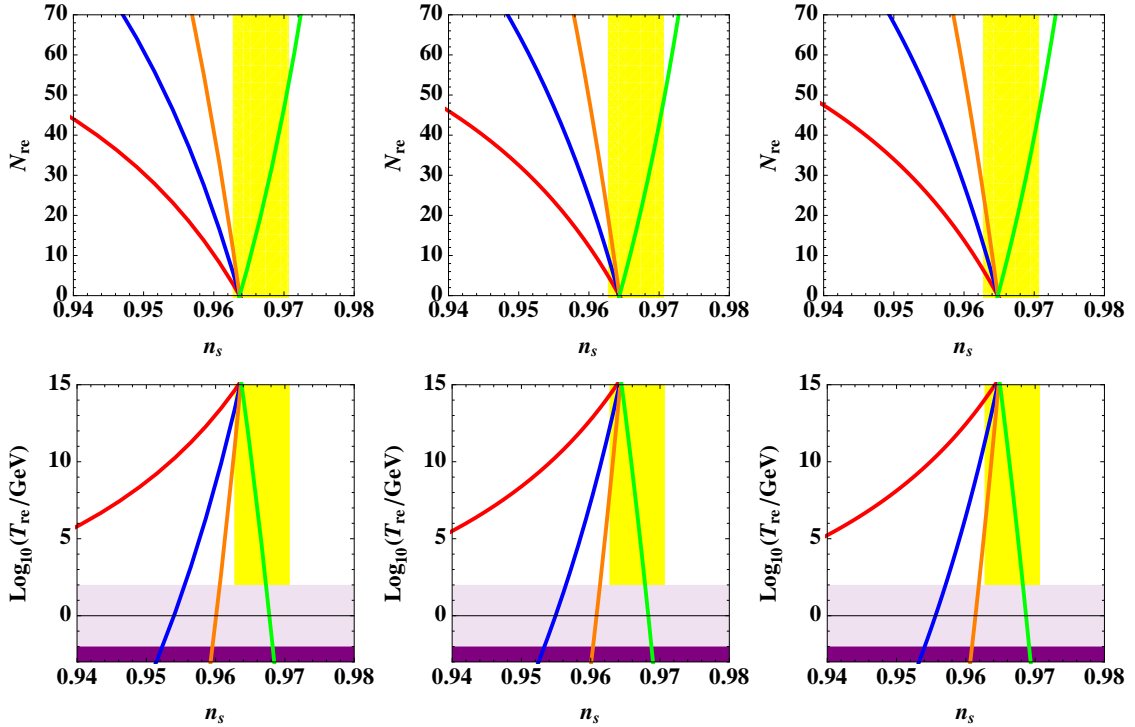


**Figure 3.** Same as figure 2 but for T-model. We fix  $n = 1$  and  $\alpha = 0.1$  (left panels),  $\alpha = 1$  (central panels), and  $\alpha = 5$  (right panels). In each panel, the curves represent different equation-of-state parameters  $w_{\text{re}}$ :  $-1/3$  (red curve),  $0$  (blue curve),  $1/6$  (orange curve), and  $2/3$  (green curve).

for the E-model and T-model, respectively, the equation-of-state parameter of the scalar field is expressed in terms of the parameter  $n$ . When the time scale of oscillation about the minimum is small, the virial theorem predicts that the energy density of the oscillating scalar field has the equation-of-state parameter

$$w_{\text{sc}} = \frac{n-1}{n+1} \quad (4.3)$$

for a potential  $V \propto \phi^{2n}$  around the minimum [26]. One can check the validity of this formula by numerical solutions for an expanding universe. This is because the period of oscillation is small compared to the Hubble time. Thus, the first oscillation phase of reheating is characterised by coherent oscillations of inflaton, in which the energy density is specified by the equation-of-state parameter  $w_{\text{sc}}$  in (4.3).

During the oscillation phase, light relativistic particles are produced gradually by a certain mechanism. We assume that the energy density of the oscillating field and the energy density of relativistic particles become equal at the scale factor  $a_{\text{eq}}$  and that the relativistic particle component dominates the energy density of the universe after  $a_{\text{eq}}$ . However, the thermalisation process might not be completed quickly. Then, the second phase of reheating is for thermalisation. We assume that the thermalisation phase continues until the scale factor becomes  $a_{\text{re}}$ , at which the temperature of the universe is  $T_{\text{re}}$  and the energy density is given by (2.11). Then, the e-folding number of the reheating epoch is written as a combination of

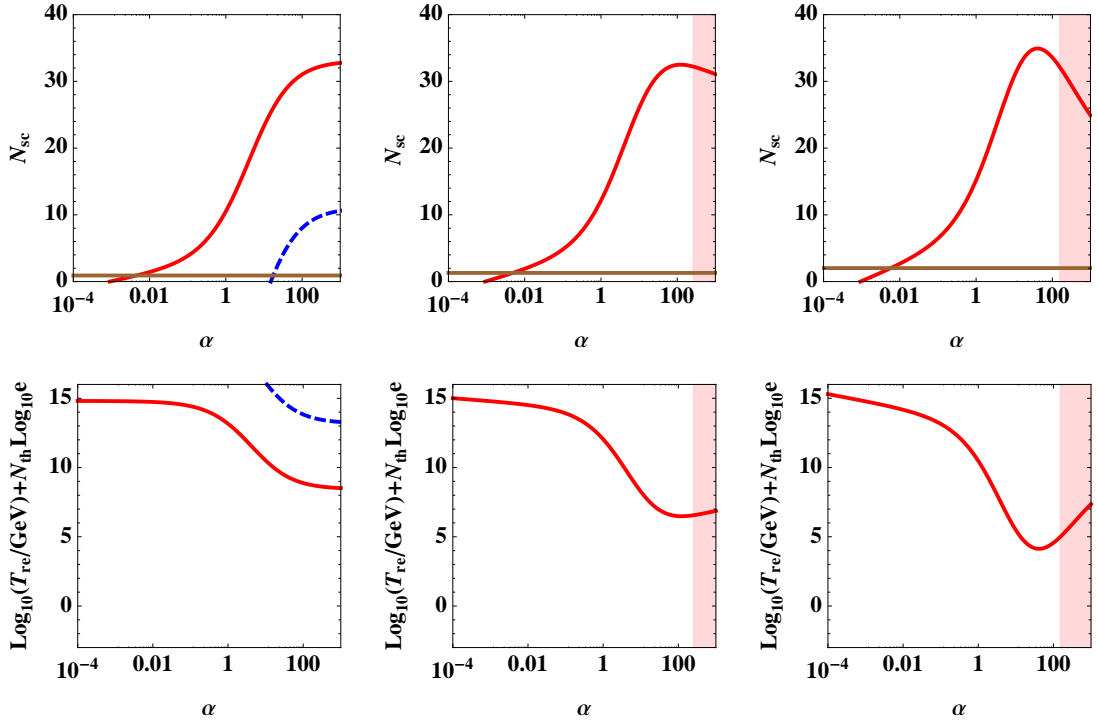


**Figure 4.** Blue curve is the maximum value of  $N_{\text{sc}}$  (upper panels) and the minimum value of  $\log_{10}(T_{\text{re}}/\text{GeV}) + N_{\text{th}} \log_{10} e$  (lower panels) as a function of  $\alpha$  for E-model with  $n = 1/2$  (left panel),  $n = 3/4$  (central panel), and  $n = 1$  (right panel). Dashed curve in left panels shows the minimum value of  $N_{\text{sc}}$  and the maximum value of  $\log_{10}(T_{\text{re}}/\text{GeV}) + N_{\text{th}} \log_{10} e$ . Brown line in upper panels shows the e-folding number for  $N_{\text{osc}} = 10$  oscillations, which is required for broad resonance preheating. Light shaded region in the central and right panels is excluded from the observational constraint on the tensor-to-scalar ratio  $r$ .

the two phases:

$$N_{\text{re}} = \ln\left(\frac{a_{\text{re}}}{a_{\text{end}}}\right) = \ln\left(\frac{a_{\text{re}}}{a_{\text{eq}}}\frac{a_{\text{eq}}}{a_{\text{end}}}\right) = N_{\text{sc}} + N_{\text{th}}, \quad (4.4)$$

where we defined

$$N_{\text{sc}} = \ln\left(\frac{a_{\text{eq}}}{a_{\text{end}}}\right) = -\frac{1}{3(1+w_{\text{sc}})} \ln\left(\frac{\rho_{\text{eq}}}{\rho_{\text{end}}}\right), \quad (4.5)$$

$$N_{\text{th}} = \ln\left(\frac{a_{\text{re}}}{a_{\text{eq}}}\right) = -\frac{1}{4} \ln\left(\frac{\rho_{\text{re}}}{\rho_{\text{eq}}}\right), \quad (4.6)$$

and  $N_{\text{sc}}$  and  $N_{\text{th}}$  are the e-folding numbers for the oscillation phase and thermalisation phase, respectively.

On the basis of this assumption, we repeat the computation in section 2, which yields

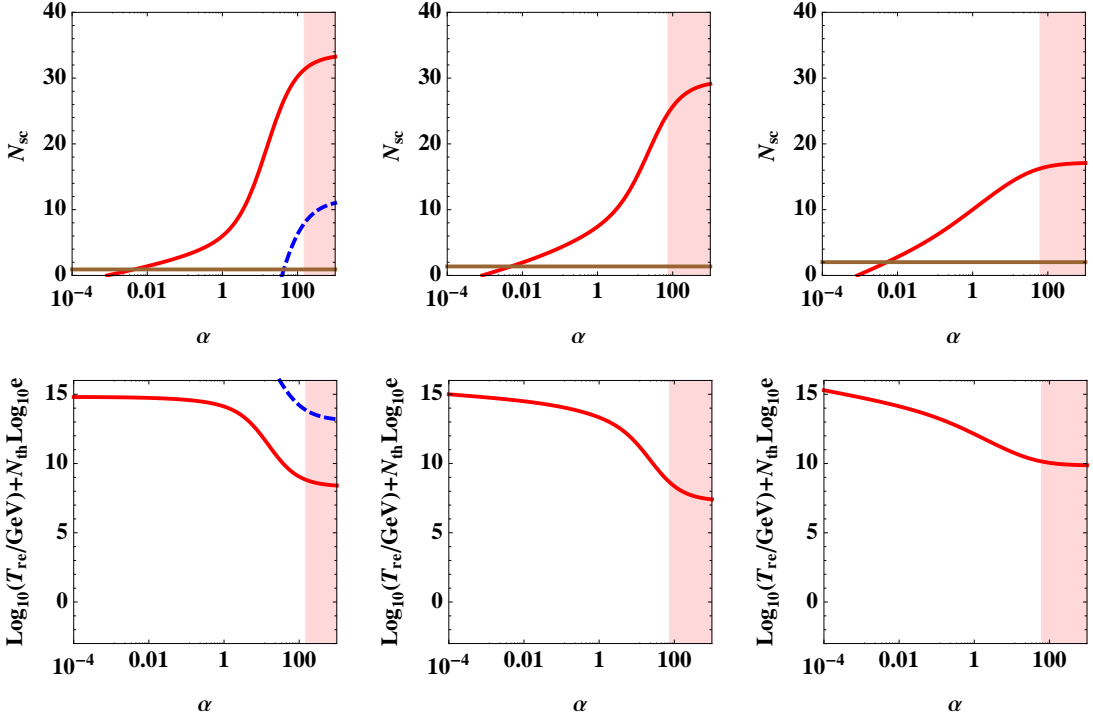


Figure 5. Same as figure 4 but for T-model.

the following expressions instead of (2.20) and (2.21):

$$N_{\text{sc}} = \frac{4}{1 - 3w_{\text{sc}}} \left[ -N_k - \ln \left( \frac{k}{a_0 T_0} \right) - \frac{1}{4} \ln \left( \frac{40}{\pi^2 g_{\text{re}}} \right) - \frac{1}{3} \ln \left( \frac{11 g_{\text{re}}}{43} \right) + \frac{1}{2} \ln \left( \frac{\pi^2 M_{\text{pl}}^2 r A_s}{2 V_{\text{end}}^{1/2}} \right) \right], \quad (4.7)$$

$$T_{\text{re}} e^{N_{\text{th}}} = \exp \left[ -\frac{3}{4} (1 + w_{\text{sc}}) N_{\text{sc}} \right] \left( \frac{2 V_{\text{end}}}{5 \pi^2} \right)^{\frac{1}{4}}. \quad (4.8)$$

Note that the expression for  $N_{\text{sc}}$  is equivalent to  $N_{\text{re}}$  in (2.20) and that the reheating temperature is modified by the e-folding number of thermalisation  $N_{\text{th}}$ , but  $T_{\text{re}} e^{N_{\text{th}}}$  is the same as the right-hand side of (2.21).

As we described in the previous section, a maximum e-folding number appears for consistency with the constraint on  $n_s$ . From (4.7), for the two-phase reheating model, we obtain the maximum e-folding number for  $N_{\text{sc}}$ , which is the same as that for  $N_{\text{re}}$ , when we fix  $\alpha$ ,  $n$ , and  $w_{\text{sc}}$  instead of  $w_{\text{re}}$ . In addition, from (4.8), we obtain the minimum reheating temperature. Note that  $T_{\text{re}} e^{N_{\text{th}}}$  in the two-reheating-phase model is the same as the right-hand side of (2.21); therefore, we obtain the minimum reheating temperature,  $\log_{10} T_{\text{re}} + N_{\text{th}} \log_{10} e$ , in this case.

Figure 4 shows the maximum value of  $N_{\text{sc}}$  (upper panels) and  $\log_{10}(T_{\text{re}}/\text{GeV}) + N_{\text{th}} \log_{10} e$  (lower panels) as functions of  $\alpha$  with  $n = 1/2$  (left panels),  $n = 3/4$  (central panels), and  $n = 1$  (right panels) for the E-model. Figure 5 is the same as figure 4 but for the T-model.

## 5 Impact on reheating scenarios

In this section, we discuss the impacts of the results in the previous section on reheating scenarios by comparing the results with theoretical predictions. We may consider two types of interaction between an inflaton field  $\phi$  and a light scalar field  $\chi$ ,

$$L_I^{(4)} = -\frac{1}{2}\tilde{g}^2\phi^2\chi^2 \quad (5.1)$$

and

$$L_I^{(3)} = -g\phi\chi^2, \quad (5.2)$$

which describe  $\chi$ -particle production through the processes  $\phi + \phi \rightarrow \chi + \chi$  and  $\phi \rightarrow \chi + \chi$ , respectively, where  $\tilde{g}$  and  $g$  are their respective coupling constants.

### 5.1 Perturbative reheating

We first consider a scenario in which effective resonant particle creation does not occur. We consider the perturbative reheating scenario as an elementary reheating scenario in which inflatons decay perturbatively through interaction (5.2). In this case, the evolution of the number density of inflatons is described by

$$\frac{d(a^3 n_\phi)}{dt} = -\Gamma_{\phi \rightarrow \chi\chi}(a^3 n_\phi), \quad (5.3)$$

where the decay rate  $\Gamma_{\phi \rightarrow \chi\chi}$ , described through the interaction in (5.2), is

$$\Gamma_{\phi \rightarrow \chi\chi} = \frac{g^2}{8\pi m_\phi}, \quad (5.4)$$

where  $m_\phi$  is the inflaton's mass. Assuming that the background universe is dominated by the energy density of inflaton oscillation, which might be treated as a fluid with the equation-of-state parameter  $w_{\text{sc}}$  in (4.3), the Friedmann equation is

$$\frac{\dot{a}^2}{a^2} = \frac{\rho_{\text{end}}}{3M_{\text{pl}}^2} \left( \frac{a}{a_{\text{end}}} \right)^{-6n/(1+n)}. \quad (5.5)$$

The above e-folding of perturbative reheating is simply understood as follows. We may estimate the epoch of  $\chi$ -particle decay as

$$H = \Gamma_{\phi \rightarrow \chi\chi}, \quad (5.6)$$

which yields

$$\left( \frac{a_{\text{eq}}}{a_{\text{end}}} \right)^{3n/(1+n)} = \frac{8\pi m_\phi}{g^2 M_{\text{pl}}} \sqrt{\frac{\rho_{\text{end}}}{3}} = \frac{16\pi m_\phi}{3g^2 M_{\text{pl}}} V_{\text{end}}^{1/2}, \quad (5.7)$$

where we used (2.9) in the second equality. We may write  $V_{\text{end}} \sim \Lambda^4 (2/3\alpha)^n$  and  $V_{\text{end}} \sim \Lambda^4 (1/6\alpha)^n$  for the E-model and T-model, respectively; then, we have the following expressions for the e-folding number, defined by  $e^{N_{\text{sc}}} = a_{\text{eq}}/a_{\text{end}}$ :

$$N_{\text{sc}} = -\frac{n+1}{3n} \ln \left[ \frac{3M_{\text{pl}}}{16\pi m_\phi} \left( \frac{g}{\Lambda} \right)^2 \left( \frac{3\alpha}{2} \right)^n \right], \quad (5.8)$$

$$N_{\text{sc}} = -\frac{n+1}{3n} \ln \left[ \frac{3M_{\text{pl}}}{16\pi m_\phi} \left( \frac{g}{\Lambda} \right)^2 (6\alpha)^n \right] \quad (5.9)$$

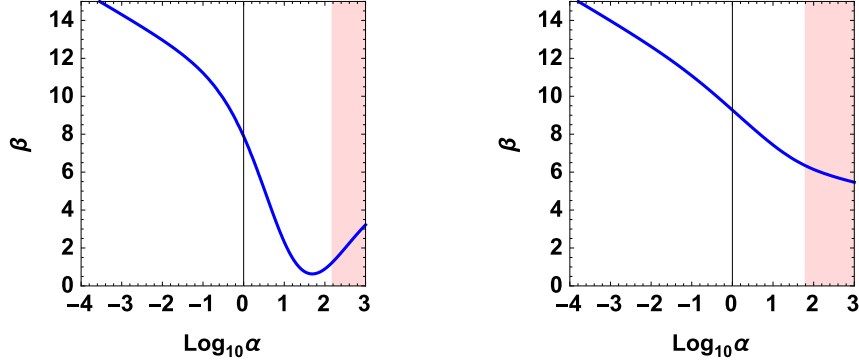


**Figure 6.** Blue curve is the minimum value of  $\beta$  for the coupling constant  $g/\Lambda = 10^{\beta-15}$  as a function of  $\alpha$  for E-model (left panel) and T-model (right panel). Here we adopted  $n = 1$  and  $m_\phi = 10^{13}$  GeV. Note that the coupling constant is defined so as to be  $g = 10^\beta$  GeV when we choose  $\Lambda = 10^{15}$  GeV.

for the E-model and T-model, respectively. This puts a useful constraint on the coupling constant  $g$  for a successful perturbative reheating scenario that is consistent with the observational constraint obtained in the previous section. When we choose  $m_\phi = 10^{13}$  GeV defining

$$\frac{g}{\Lambda} = 10^{\beta-15}, \quad (5.10)$$

we have

$$\beta \gtrsim 12.9 - n\gamma - 0.65 \frac{n}{n+1} N_{\text{sc}} - \frac{n}{2} \log_{10} \alpha \quad (5.11)$$

where  $\gamma = 0.088$  and  $\gamma = 0.39$  for the E-model and T-model, respectively. Figure 6 shows the minimum value of  $\beta$  as a function of  $\alpha$  for the E-model (left panel) and T-model (right panel) with  $n = 1$ . For example,  $\beta > 7.8$  for the E-model with  $\alpha = 1$  and  $\Lambda = 10^{15}$  GeV. For the T-model with  $\alpha = 1$  and  $\Lambda = 10^{15}$  GeV, for successful perturbative reheating,  $\beta > 9.2$  is imposed.

## 5.2 Broad resonance preheating

After the end of slow-roll inflation, the inflaton field  $\phi$  oscillates around a potential minimum, which is assumed to be approximated by (4.1) and (4.2) for the T-model and E-model, respectively. When  $n = 1$ , these potentials are the harmonic potential, and we may assume that the oscillation of  $\phi(t)$  is approximated by

$$\phi(t) \simeq \Phi \sin m_\phi t, \quad (5.12)$$

where  $\Phi$  is the amplitude of the oscillation, and  $m_\phi$  is understood as  $m_\phi = \Lambda^2/3M_{\text{pl}}$  and  $m_\phi = 4\Lambda^2/3M_{\text{pl}}$  for the T-model and E-model, respectively. When  $n \neq 1$ , the oscillation of  $\phi(t)$  is not approximated by such a simple function.

We here consider a resonant particle production scenario that was intensively investigated by Kofman, et al. [23] (see also [24]). The equations of motion for a Fourier mode of the  $\chi$  field are

$$\ddot{\chi}_k(t) + 3\frac{\dot{a}}{a}\dot{\chi}_k(t) + \left( \frac{k^2}{a^2} + m_\chi^2 + \tilde{g}^2\phi^2(t) \right) \chi_k = 0 \quad (5.13)$$

and

$$\ddot{\chi}_k(t) + 3\frac{\dot{a}}{a}\dot{\chi}_k(t) + \left(\frac{k^2}{a^2} + m_\chi^2 + g\phi(t)\right)\chi_k = 0 \quad (5.14)$$

for the interactions in (5.1) and (5.2), respectively.

This scenario of reheating relies on resonant particle creation due to the periodic time-dependent background at the earlier stage of reheating, which is called preheating. Particle creation effectively occurs when the Wentzel–Kramers–Brillouin approximation breaks down, which occurs at  $\cos 2m_\phi t \sim 0$  or  $\sin m_\phi t \sim 0$ , depending on the interaction. We follow this scenario (see [9] for a review). We first consider the four-point interaction. After  $\mathcal{N}_{\text{osc}}$  oscillations of inflaton field around the minimum, the ratio of the number density of  $\chi$  particles to that during inflaton is estimated as

$$\frac{n_\chi}{n_\phi} \sim \frac{k_*^3 n_k(\mathcal{N}_{\text{osc}})}{\frac{1}{2} m_\phi \Phi_0^2} \sim m_\phi^{1/2} \tilde{g}^{3/2} 3^{\mathcal{N}_{\text{osc}}} \Phi_0^{-1/2}, \quad (5.15)$$

where we choose  $k_* = m_\phi^3 (\tilde{g}\Phi_0/m_\phi)^{3/2}$ , and  $\Phi_0$  is the inflaton's oscillation amplitude, which we take to be  $\Phi_0 \sim M_{\text{Pl}}$ . Using this relation, we can estimate the ratio of the energy density of  $\chi$  particles to that during inflation as

$$\frac{\epsilon_\chi}{\epsilon_\phi} \sim \frac{m_\chi n_\chi}{m_\phi n_\phi} \sim \tilde{g}^{5/2} m_\phi^{-1/2} \mathcal{N}_{\text{osc}}^{-1} 3^{\mathcal{N}_{\text{osc}}} \Phi_0^{1/2}, \quad (5.16)$$

where we assumed  $m_\chi = \mathcal{O}(m_\phi) = \mathcal{O}(\tilde{g}\Phi) \sim \tilde{g}\Phi_0/\mathcal{N}_{\text{osc}}$ . Then  $\epsilon_\chi \simeq \epsilon_\phi$  appears after  $\mathcal{N}_{\text{osc}}$  oscillations,

$$\mathcal{N}_{\text{osc}} \simeq 6 \sim 15, \quad (5.17)$$

for a wide range of  $10^{-5} < \tilde{g} < 10^{-3}$ , where we assumed  $m_\phi = 10^{13}$  GeV. Here we compute the e-foldings to realise  $\mathcal{N}_{\text{osc}} = 10$  inflaton oscillations; this yields the minimum duration required for successful preheating. The e-folding number for  $\mathcal{N}_{\text{osc}} = 10$  oscillations is of order  $\mathcal{O}(1 \sim 2)$ . Then we may write  $N_{\text{sc}} \gtrsim \mathcal{O}(1 \sim 2)$ . A more explicit value is obtained by solving (2.1) and (2.2). The brown line in the upper panels of figures 4 and 5 shows the value of  $N_{\text{sc}}$  for a broad resonance preheating scenario with  $\mathcal{N}_{\text{osc}} = 10$ . For the interaction in (5.2), the estimation is essentially the same as the above estimation of the interaction in (5.1).

When we also consider the constraint in the previous section, for consistency with the broad resonance preheating scenario, we need the rough condition

$$\alpha \gtrsim 0.01. \quad (5.18)$$

## 6 Summary and Conclusions

We investigated a constraint on the reheating epoch using an observational constraint on the spectral index  $n_s$ , in which we assumed the E-model and T-model as generalised  $\alpha$ -attractor models of inflation. When the reheating epoch is dominated by an energy component of the cosmic equation-of-state parameter  $w_{\text{re}}$ , the e-folding number for reheating,  $N_{\text{re}}$ , is bounded depending on  $w_{\text{re}}$ , which also limits the reheating temperature  $T_{\text{re}}$ . Assuming that the reheating consists of two phases, an oscillation phase and a thermalisation phase, we investigated

the e-folding number of the oscillation phase  $N_{\text{sc}}$  and the reheating temperature  $T_{\text{re}}$ , depending on the equation-of-state parameter  $w_{\text{sc}}$ , which is determined by the potential.  $N_{\text{sc}}$  is constrained by the observational constraint on  $n_s$ , and the allowed regions of  $N_{\text{sc}}$  and  $T_{\text{re}}$  were obtained in section 4. For example, we found  $N_{\text{sc}} \lesssim 16$  and  $T_{\text{re}} e^{N_{\text{th}}} \gtrsim 10^{10} \text{ GeV}$  for the E-model with  $n = 1$  and  $\alpha = 1$ , whereas  $N_{\text{sc}} \lesssim 10$  and  $T_{\text{re}} e^{N_{\text{th}}} \gtrsim 10^{12} \text{ GeV}$  for the T-model with  $n = 1$  and  $\alpha = 1$ . We discussed the implications of our results for two simple reheating scenarios. For the simplest perturbative reheating scenario, the ratio of the coupling constant  $g$  for a decay to the mass scale of the potential of inflation  $\Lambda$  should be  $g \gtrsim 10^{7.8} (\Lambda/10^{15} \text{ GeV})$  GeV for the E-model and  $g \gtrsim 10^{9.2} (\Lambda/10^{15} \text{ GeV})$  GeV for the T-model for  $n = 1$  and  $\alpha = 1$ . Along a broad resonance preheating scenario, the  $\alpha$  parameter is roughly constrained,  $\alpha \gtrsim 0.01$ , for the T-model and E-model.

## Acknowledgment

This work was supported by MEXT/JSPS KAKENHI Grant Number 15H05895.

## References

- [1] Planck Collaboration: P. A. R. Ade et al., arXiv:1502.02114
- [2] R. Kallosh, A. Linde, JCAP 06(2013)028
- [3] R. Kallosh, A. Linde, JCAP 07(2013)002
- [4] R. Kallosh, A. Linde, D. Roest, JHEP 11(2013)198
- [5] R. Kallosh, A. Linde, JCAP 06(2013)027
- [6] R. Kallosh, A. Linde, JCAP 10(2013)033
- [7] M. Galante, R. Kallosh, A. Linde, D. Roest, Phys. Rev. Lett. **114** 141302 (2015)
- [8] A. A. A. Starobinsky, Phys. Lett. **B91** 99 (1980)
- [9] V. F. Mukhanov, G. V. Chivisov, JETP Lett. **33** 532 (1981)
- [10] H. Nariai, Prog. Theor. Phys. **46** 433 (1971)
- [11] H. Nariai, K. Tomita, Prog. Theor. Phys. **46** 776 (1971)
- [12] H. Nariai, Prog. Theor. Phys. **49** 165 (1973)
- [13] H. Nariai, Prog. Theor. Phys. **51** 613 (1974)
- [14] D. S. Salopek, J. R. Bond, J. M. Bardeen, Phys. Rev. D **40** 1753 (1989)
- [15] F. L. Bezrukov, M. Shaposhnikov, Phys. Lett. **B659** 703 (2008)
- [16] N. Okada, M. U. Rehman, Q. Shafi, Phys. Rev. D **82** 043502 (2010)
- [17] F. Bezrukov, D. Gorbunov, JHEP 07(2013)140
- [18] A. Linde, M. Noorbala, A. Westphal, JCAP 03(2011)013
- [19] L. F. Abbot, E. Farhi, M. B. Wise, Phys. Lett. **B117** 29 (1982)
- [20] A. D. Dolgov, A. D. Linde, Phys. Lett. **B116** 329 (1982)
- [21] A. J. Albrecht, P. J. Steinhardt, M. S. Turner, F. Wilczek, Phys. Rev. Lett. **48** 1437 (1982)
- [22] J. H. Trancshen, R. H. Brandenberger, Phys. Rev. D **42** 2191 (1990)
- [23] L. Kofman, A. D. Linde, A. A. Starobinsky, Phys. Rev. Lett. **73** 3195 (1994)

- [24] Y. Shtanov, J. H. Traschen, R. H. Brandenberger, Phys. Rev. D **51** 5438 (1995)
- [25] L. Kofman, A. D. Linde, A. A. Starobinsky, Phys. Rev. D **56** 3258 (1997)
- [26] V. F. Mukhanov, Physical Foundations of Cosmology, (Cambridge University Press, 2005)
- [27] R. Allahverdi, R. Brandenberger, F.-Y. Cyr-Racine, A. Madumder, Ann. Rev. Nucl. Part. Sci. **60** 27 (2010)
- [28] M. A. Amin, M. P. Hertzberg, D. I. Kaiser, J. Karouby, Int. J. Mod. Phys. D **24** 1530003 (2015)
- [29] L. Dai, M. Kamionkowski, J. Wang, Phys. Rev. Lett. **113** 041302 (2014)
- [30] J. B. Unoz, M. Kamionkowski, Phys. Rev. D **91** 043521 (2015)
- [31] J. L. Cook, E. Dimastrogiovanni, D. Easson, L. M. Krauss, JCAP 04(2015)047
- [32] J. J. M. Carrasco, R. Kallosh, A. Linde, JHEP 10(2015)147
- [33] J. J. M. Carrasco, R. Kallosh, A. Linde, Phys. Rev. D **92** 063519 (2015)
- [34] Planck Collaboration: P. A. R. Ade et al., arXiv:1502.01589